

## **Influence of the nature of the synthetic incorporated fibres in UHPFRC when subjected to fire conditions**

**Evariste Ouedraogo (1), Yann Malecot (1), Ludovic Missemmer (1, 2), Christian Clergue (2) and Damien Rogat (2)**

(1) Laboratoire 3SR, UJF-Grenoble 1, Grenoble INP, CNRS UMR 5521, Grenoble, France

(2) Sigma-Beton Vicat, L'Isle d'Abeau, France

### **Abstract**

The study focuses on the knowledge on the fire behaviour of an Ultra High Performance Concrete in formulations without or with polypropylene or acrylic fibres of different dosages. Blowtorch tests showed that formulations with acrylic fibres exhibited spalling for important dosages unlike formulations with polypropylene fibres which exhibited spalling for dosages significantly lower. Analyses of the SEM micrographs showed that the network of micro-cracks around the beds of polypropylene fibres was denser than around acrylic ones and, on the other hand, polypropylene when spraying left completely the fibre beds unlike acrylic ones. Through analysis of mercury porosimetry measurements, one could highlight a criterion called critical zone factor that allows the discrimination of the fire resistant formulations from the others.

### **Résumé**

L'étude porte sur la connaissance du comportement au feu d'un Béton à Ultra Hautes Performances dans une formulation sans fibres et dans des formulations comportant des fibres de polypropylène et d'acrylique de différents dosages. Des essais au chalumeau ont montré la forte tendance à l'éclatement des formulations à base de fibres d'acrylique contrairement à celles à base de fibres de polypropylène pour un dosage équivalent. Des analyses de micrographies au MEB ont montré : que le réseau de microfissures autour des lits de fibres de polypropylène était plus dense que celui autour des fibres d'acrylique et que le polypropylène en se vaporisant libérait complètement les lits de fibre contrairement à l'acrylique. Par l'analyse des mesures de porosimétrie au mercure, on a pu mettre en évidence un critère, appelé facteur de zone critique, qui a permis de discriminer les différentes formulations étudiées vis-à-vis de l'écaillage.

## **1. INTRODUCTION**

The Ultra High Performance Concretes are characterized by a compressive strength greater than 150 MPa. This exceptional performance is achieved by action at the level of the microstructure, in particular maximizing their compactness by adding fine particles of inorganic filler, fine powder of quartz and silica fume [1, 2]. This compactness reduces their capillarity and thus makes the concrete more susceptible to explosive fragmentation (spalling)

that is one of the most dangerous damage mechanisms for structures built with these materials. Studies [3, 4] showed that the higher the compressive strength reached the more intense will be the spalling phenomenon. Thus, two main mechanisms are commonly invoked to explain the phenomenon of spalling of concrete under the action of temperature: the presence of a temperature gradient and movement upset the water vapor in the material. In the first case argued by [5, 6], the appearance of a thermal gradient caused by fire exposure is such that the stress state reaches the breaking point and causes a rupture that can spread and lead to spalling. The second mechanism, known as the 'moisture clog', is due to partial saturation of water in concrete [3]. The water in the concrete, in free or bound form, is vaporized due to the increase of temperature. Steam close to the wall is removed by it while the deep-seated is forced to migrate inwards. The material heart is colder; the vapor condenses thereby increasing the degree of saturation of unsaturated pores encountered. One can imagine that at some point an impermeable barrier stands. Vapor pressure then increases to the point that in some areas the tension limit is reached leading to fracture. These mechanisms are borderline cases and it is commonly accepted that these two mechanisms act in concert to produce the phenomenon of spalling [7, 8].

A well-known solution to improve the temperature behavior of concrete is to add cylindrical polypropylene fibers [9-15]. Although experience shows their effectiveness, efficiency mechanisms behind this are still under investigation. The purpose of this study is to improve the fire performance of ultra high performance fiber-reinforced concrete (BCV) by performing tests on various formulations obtained with different fibers and with a polypropylene powder. We seek through this study to understand the mechanisms explaining why some fibers are effective, especially why they are more effective than others. We will focus on formulations based on polypropylene powder or fiber and on acrylic fibers.

## 2. MATERIALS AND MODALITIES

In this chapter information about the studied materials is given. A basic concrete formulation without fibers is used as a reference for defining new formulations with fibers by varying their nature and their dosage. The details are given below.

### 2.1 The basic formulation

The studied material is based on the matrix of a specific ultra high performance fiber-reinforced concrete called BCV (Béton Composite Vicat). This concrete that can be considered as a mortar is composed of silica sand ( $d / D = 0/2$  mm), Vicat cement CEM I, silica fume, water and superplasticizer (see Table 1). Cement paste has a low water / binder ratio that gives to the concrete exceptional performance in terms of mechanical properties. To increase the ability to use in structures, steel metal fibers 13 and 20 mm length are incorporated to increase the tensile strength of the material.

Table 1: Concrete composition

Constituents	kg.m <sup>-3</sup>
Mixture (sand, cement and silica fume)	2085.6
Superplasticizer	28.7
Water	194
W/B ratio	0.19

The studied concrete is constituted of the same elements as the BCV (without the metal fibers) added with synthetic fibers of different dosages to obtain various formulations. The study deals with the determination of the spalling resistance of the BCV matrix without metal fibers, when synthetic fibers of different types and in different quantities are added. In this study only the results for polypropylene fibers (PP) and those of acrylic (PAN) will be presented. Let's examine now their physico-chemical characteristics.

## 2.2 Incorporated synthetic fibers

For polypropylene (PP), two fiber sizes (12 mm long – 33  $\mu\text{m}$  diameter and 6 mm long - 18  $\mu\text{m}$  diameter) provided by Bekaert and one spherical size of a Micronal powder ((M, 20  $\mu\text{m}$  diameter) were selected. With this variety it would be possible to highlight the influence of the fiber geometry. For acrylic fibers, only fibers with dimensions 6 mm long and 14  $\mu\text{m}$  diameter were used. To characterize the thermal behavior of these fiber standard thermogravimetric analysis (TGA) and differential scanning calorimetry (DSC) tests and non-standard heating tests were carried out on the fiber materials.

Fig. 1 displays the results for polypropylene. The DSC curve shows several peaks, the temperature of 166.4°C corresponding to the melting temperature of the polypropylene evidenced by the small variation of the TGA curve in this temperature range. The curve of mass loss (TGA) shows a strong variation between 250 and 350°C from 100 to 10%. The DSC curve shows a peak around 300°C, median temperature of the range mentioned above. This strong variation corresponds to the phenomenon of sublimation, vaporization of polypropylene. It can be seen that at 500°C, the polypropylene is quasi-completely vaporized. Corresponding curves for acrylic (not shown here) are quite different. The first peak is exothermic and occurs at 311 °C followed by a second small peak at 329 °C. These peaks recorded on the DSC curves are correlated with a significant change in mass on the TGA curve that was not observed on polypropylene. The change in mass of the acrylic occurs in two stages: a first moderate variation between 300 and 450°C followed by a much larger variation between 450 and 700°C, temperature at which all the material is vaporized.

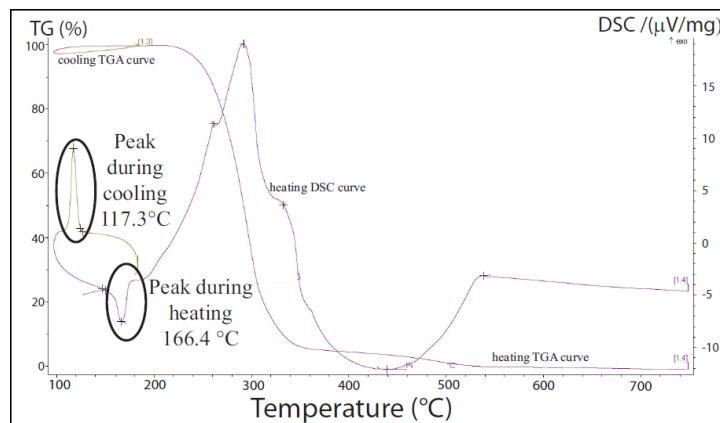


Figure 1: TGA and DSC curves of Polypropylene (PP).

The non-standard test undertaken consisted in heating the container of polypropylene or acrylic fibers at defined temperatures and removing it in order to make observations in hot conditions. A temperature rate of 10°C / min was applied and the observations made at 25,

220 and 380°C temperatures. These tests showed that at 220°C the polypropylene fibers were melted and formed a liquid bath and that at 380°C they have quasi-totally vaporized. In the case of acrylic, a liquid phase was not really observed at the characteristic melting temperature but one cluster in agglutination as the temperature increases. Hence, the temperature of 311°C observed on the DSC curve of the acrylic is not a melting temperature in itself as for polypropylene but corresponds to a degradation mechanism evidenced by the change in TGA mass curve. In summary, the melting temperature and the temperature range of degradation of polypropylene is lower than acrylic (166°C / 250-300°C against 311°C / 450-700°C, respectively).

### 2.3. The studied formulations

Sample preparation followed a strict protocol defined in advance [16]. After mixing all solid components, water and liquid components were added to the mixture in steps where the mixing speed and durations changed. Once the mixture of the required quality was obtained, the concrete was poured into molds which were then covered by a plastic film for 24 hours. Specimens manufactured for torch flame tests were stocked in a particularly humid atmosphere to increase their risk of spalling. They were kept for 28 days at a humidity of 90 %. They were then taken out 24 hours before testing and kept in an atmosphere with a humidity level less than 50% in order to dry their faces.

The nature, amount and characteristics of fibers added to concrete for the various studied formulations are given in Table 2. The letter C denotes the formula without synthetic fibers used as a reference.

Table 2: Characteristics of the formulations presented in this study

Formulation	Addition Type	Fibre length mm	Diameter $\mu\text{m}$	Fibre content $\text{kg.m}^{-3}$	Specific area $\text{m}^2.\text{m}^{-3}$
C	None	--	--	--	--
CPP1	PP	6	18	3.27	800
CPP2	PP	12	33	3	400
CPP3	PP	12	33	4.5	600
CPAN	PAN	6	14	3.22	800
CM	PP	--	20	65.73	21800

## 3. DESCRIPTION OF THE TESTS

### 3.1 Blowtorch tests

All compositions given in Table 2 were subjected to blowtorch tests. Prismatic specimens of length 80 mm and square section 40 mm x 40 mm were used. A physical view of the test is shown in Fig. 2. This test is not standardized and doesn't take into account structure scale effect; however, it can easily distinguish the different concrete compositions vis-à-vis their resistance to spalling. Some of the test specimens were equipped with a thermocouple; the bent end initially palpates the middle of the exposed surface of the specimen. It was then possible to measure continuously the temperature during the test. An infrared pointing at the face of the specimen gave additional redundant information on the temperature. Finally, a video camera, placed far enough from the installation to avoid splashing, could shoot test and

detect the timing and extent of the outbreak occurred. The tests lasted 5 min. The specimen was first placed at 15 cm from the torch. If the burst occurred, it was assumed that the breakup would occur at  $d = 10$  cm since the conditions are more severe in this location. If the break was not observed, the test was restarted at 10 cm on the other blank side of the specimen.

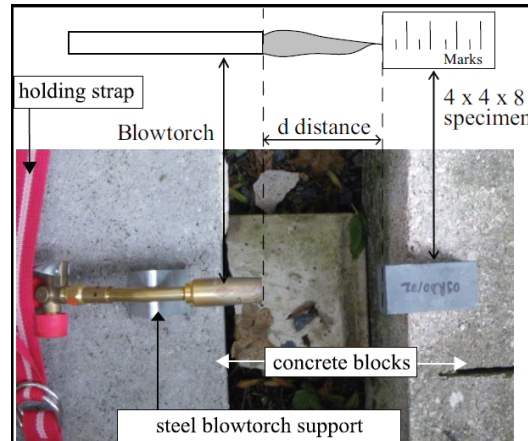


Figure 2: Sketches and side view of the test facility for the torch distance of 10 cm.

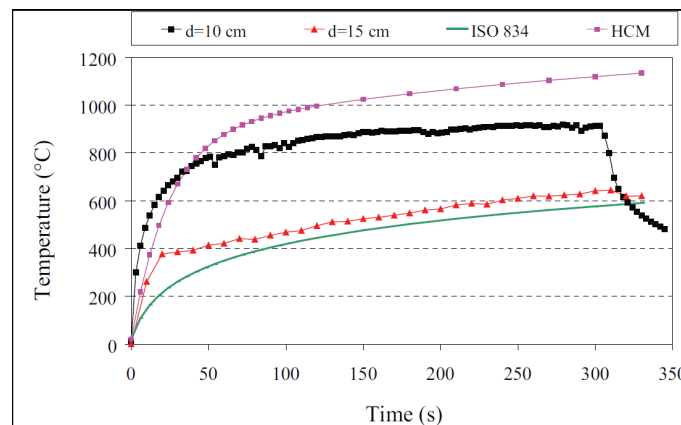


Figure 3: Evolution of temperature versus time during a blowtorch test for distances of 10 and 15 cm compared to standard curves ISO834 and HCM.

Fig. 3 shows the experimental curves of temperature evolution with time measured at 10 and 15 cm and the standard curves in case of building fire (ISO834) or fire in presence of hydrocarbons (HCM). Globally the experiment are “more severe” at the beginning than standards and then tend to converge ( $d = 15$ cm) to ISO834 or diverge ( $d = 10$  cm) from HCM. This figure is aimed to compare the non-standard proposed test to standards.

### 3.2 Scanning electron microscopy (SEM) analysis

This type of analysis allows precisely access to the knowledge on concrete at microstructure level. To obtain good quality images, it is preferable to make measurements at room temperature using the technique of backscattered electron capture (BESD), which allows a contrast correlated to the atomic number of the element: the higher the atomic

number the clearer the obtained images. This allows particularly high contrast that makes visible defects such as cracks or micro-cracks in concrete. To conduct the analysis of SEM samples, of 1 cm characteristic size, were taken from the 40 mm x 40 mm x 160 mm specimens. They are then stored in a conditioning chamber (20°C, 50 % RH) until they undergo thermal cycling and SEM analyzes. The samples were first heated in the following three-step thermal cycle: heating up to 110, 170, 200, 280, or 350°C temperatures, then held at the target temperature for 2 h, then cooled down to room temperature. Once at room temperature, the sample can then be placed in the SEM for the micrographic observations. A special positioning device allowed an exact positioning of the sample in order to observe the same area from a temperature to another after each manipulation.

### **3.3 Mercury intrusion porosimetry**

This technique is used to access the pore size and its distribution in the concrete since it remains intrinsically a porous material. The issues are: the pore size and their distribution, evolution with temperature, possible connectivity. Samples of dimensions (1 cm x 1 cm x 2cm) were taken from prismatic samples and heated in a furnace at 50°C and at a moisture content of 8 % for 1 month in order to reduce the amount of free water without damaging the material. Reproducibility tests have ensured that the cutting conditions of the samples had a negligible influence on the results. Several tests were conducted to measure the influence of the heating temperature on the porosity of the concrete. Tests were carried out on formulations containing polypropylene fibers 12 mm long and previously heated to 150, 350 or 500°C before being cooled. The results showed that the influence of the heating temperature is established: the overall porosity increases with the increasing heating temperature. A reference temperature of 350°C was chosen and the results of the studied formulations are given in Table 3, where 'C' represents the concrete paste without fibers.

From the tests of mercury intrusion porosimetry, the distribution of pores as a function of the applied pressure of mercury is given and displayed. There are models based on simplified assumptions heavy enough that convert pressure distribution of the mercury to pore size. However, this type of model being fed controversy and criticism of any kind [17] which we seem justified in many ways, we'll just keep the mercury applied pressure in abscissa of the curves presented in this study.

## **4. RESULTS AND DISCUSSION**

### **4.1 Blowtorch Tests**

These tests were carried out on the different formulations and results are given in Table 4. Only formulations CPP1 and CPP3 resisted spalling at the two distances, the others did not resisted to any of the distances. Of the two formulations that resisted, CPP1 comprises fibers  $\phi 12 \mu\text{m}$ -6 mm at a dosage of 3.27 kg/m<sup>3</sup> and CPP3 comprises fibers  $\phi 33 \mu\text{m}$ -12 mm at a higher dosage of 4.5 kg/m<sup>3</sup>. Although formulation CPP2  $\phi 33 \mu\text{m}$ -12 mm had a dosage of the same order as the CPP1 (3 kg/m<sup>3</sup>), it did not survive, probably reflecting the influence of the specific surface area that is greater for the fibers of formulation CPP1 ( $\phi 12 \mu\text{m}$ -6 mm) than for the one of CPP2 ( $\phi 33 \mu\text{m}$ -12 mm). We also note that the Micronal (CM) which specific surface area and dosage levels are very important did not resist bursting. This highlights the influence of particle shape, particle type fibers (CPP1, CPP2 and CPP3) tending to create a

percolating network and facilitate the removal of water vapor in contrast to spherical particles (CM). To increase the resistance to spalling, additions of powder type are to be avoided.

Table 3: Blowtorch tests results for different formulations

Formulation Name	Fibres dosage kg.m <sup>-3</sup>	Specific Area m <sup>2</sup> .m <sup>-3</sup>	Spalling d=10 cm	Spalling d=15 cm
C	--	--	YES	YES
CPP1	3.27	800	NO	NO
CPP2	3	400	*	YES
CPP3	4.5	600	NO	NO
CPAN	3.22	800	*	YES
CM	65.73	21800	*	YES

\* Undone test.

#### 4.2 Analysis in a scanning electron microscope (SEM)

The results presented deal with some observations made on a resistant formulation based on polypropylene (PP) fiber and a non-resistant formulation based on acrylic (PAN) fibers. We look for SEM observations to find evidence to explain the difference in their behavior vis-à-vis the break. Fig. 4 and 5 are micrographs of concrete mixtures containing PP or PAN fibers, respectively, depending on the heating temperature. The repositioning device has been used with success. In Fig. 4, we can clearly see the network of micro-cracks present at room temperature and becoming increasingly dense as the temperature increases from 25 to 350°C. Most of the micro-cracks pass through the beds of fibers while others bypass the aggregates.

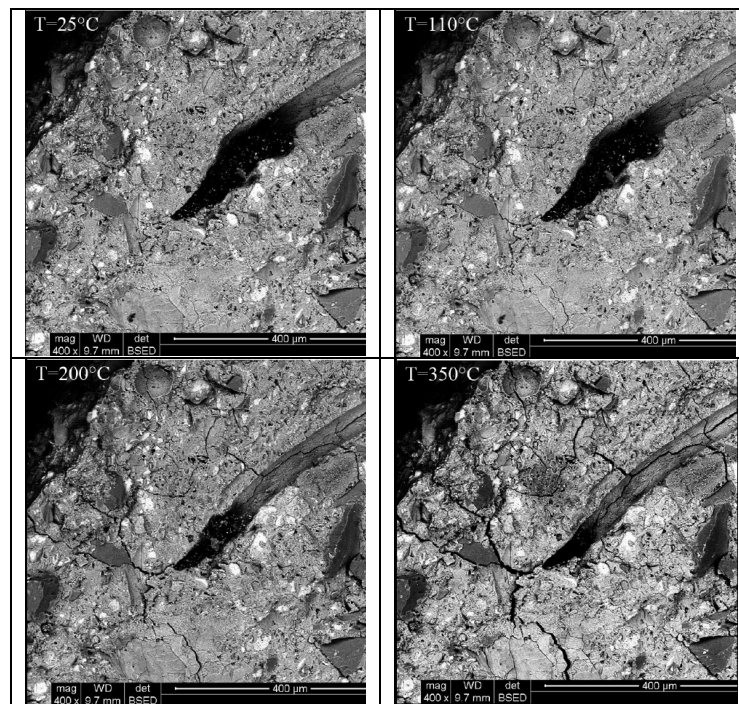


Figure 4: BSED micrographs showing the development of cement paste around a polypropylene fiber at 25, 110, 200 and 350°C.

The comparison of Fig. 4 and 5 shows a larger number of cracks through the beds of polypropylene PP fibers (Fig. 4) than those of acrylic fibers PAN (Fig. 5). The potential crack networks constituted by the fibers beds once evaporated are more connected to the crack network initially present in the case of polypropylene fibers than for acrylic fibers. This is the first part of the explanation. To go further we did a zoom on the beds of PP and PAN fibers.

The observations showed apparently that the beds of polypropylene fibers once evaporated are fully open and fully visible as micro-cracks while in the case of acrylic fibers, plastic film would cover the bed and thus obstruct cracks through the beds of fibers. Under these conditions, the water vapor would be more difficult to escape in the latter case than in the former. The explanation for this phenomenon is quite delicate. It is known from Khoury [9] as polypropylene is highly hydrophobic which means that it has no particular affinity to adhere to the cement paste during drying which is involved in dehydration. At temperature of 350°C, polypropylene fibers have widely sprayed and the non-standard tests mentioned above showed that this evaporation is effective. At this temperature, the acrylic has just begun to evaporate; it is a temperature where it is viscous and might have a tendency to stick, what could explain the presence of the film that has been observed. In other terms, Acrylic would be less hydrophobic than polypropylene or more hydrophilic at this temperature range.

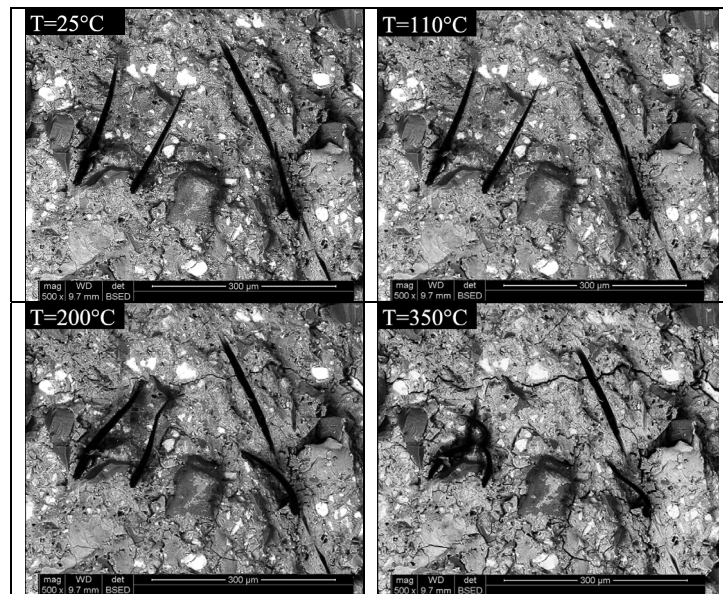


Figure 5: BSED micrographs showing the development of cement paste around acrylic fibers at 25, 110, 200 and 350°C.

#### 4.3 Mercury intrusion porosimetry

The purpose of the mercury porosimetry studies is an attempt to correlate the phenomenon of spalling to a microstructure parameter, namely the pores and their distribution in the material. The samples used for these measurements were first heated at a rate of 10°C / min up to the target temperature, and then maintained at this temperature for 2 hours before undergoing a cooling phase.

We show in Fig. 6 the total porosity measured for the different studied formulations. We can notice that the Micronal (CM) has the highest global porosity (16.2 %) and the

formulations CPP2, CPAN and concrete alone (C) have porosities neighboring the order of 12 %. CPP1 formulation that has resisted to blowtorch tests has a porosity of 13.4 %. If we consider all the compositions, the overall porosity is not a sufficient parameter to determine whether a material is likely to spall or not. But considering only compositions with fiber, this seems to be the case.

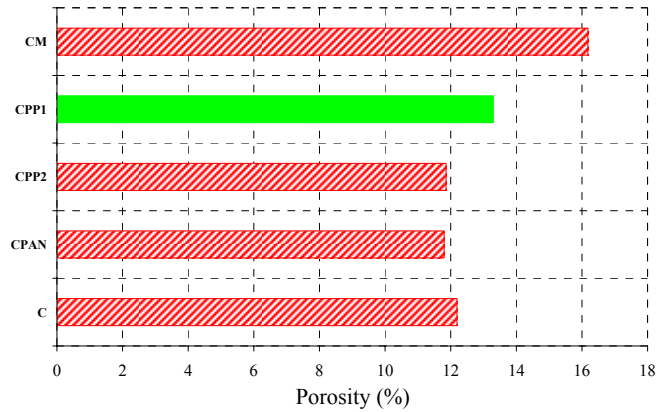


Figure 6: Total porosity of the presented formulations: solid area indicates that the composition has stood the flame test and the hatched area otherwise.

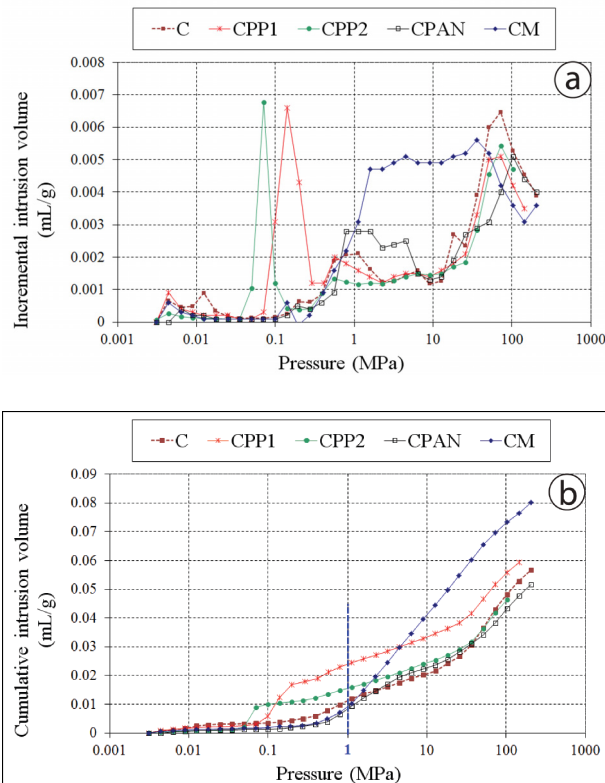


Figure 7: Porosity distribution for the studied formulations: a- incremental intrusion volume  
 b- cumulative intrusion volume

We then tried to find a better criterion to discriminate formulations vis-à-vis their resistance to spalling. It has been then reported in Fig. 7 the curves of incremental volume and cumulative volume of the various formulations. One can see on the figure of the incremental volume that connectivity varies greatly depending on the formulations, notable for CPP formulation and low for others. Especially the disappearance of PP fibers creates a peak which corresponds approximately to the diameter of fibers. This melting of the fibers also allows creating connectivity between the two areas highlighted pores at room temperature. We can see that the disappearance of PAN fibers is not as pronounced as that of PP. It may be noticed that the PP powders 'CM' generate a new zone pore, the small pores corresponding to a pressure greater than 1 MPa, which suggests that this pressure is a good limit to discriminate the different formulations vis-à-vis the spalling. The choice of this pressure value only based on the obtained results needs to be further justified on physical basis. As pore pressure is one of the driving forces of concrete spalling, an attempt should be made to link the pressure value to the surface tension of water or to the tensile resistance of the matrix.

Liu et al. [15] have shown the importance of connectivity created by the merger of polypropylene fibers in improving the fire resistance of concrete. In our case, we want to discriminate between the two formulations CCP1 and CPP2 which correspond to different fiber sizes. To define an indicator capable of representing the connectivity between micro and macro pores, it was considered the area under the curve of incremental volume and limited by the value of 1 MPa. In other words this indicator is the value obtained at the pressure 1 MPa on the curve of cumulative volume. This indicator is called critical zone factor and noted Fzc.

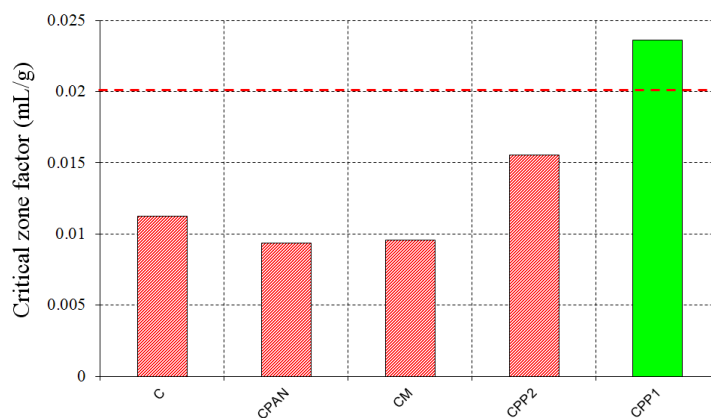


Figure 8: Critical values for each of the compositions.

These results are shown in Fig. 8 where we can observe a better differentiation of formulations that have stood (full area) from others (hatched area). From this figure we set the limit value Fzc to 0.2 ml / g.

This new indicator implies that the value of the cumulative volume must be sufficiently high at 1 MPa intrusion pressure and therefore the small pores would have a negligible influence on the resistance in the flame test. The proposed procedure for accessing this factor is more direct than conducting fire tests on real elements, which makes this an innovative approach in the prediction of spalling.

## 5. CONCLUSION

In this study spalling tests with the use of a blowtorch were developed. Different formulations of concrete without or mixed with fibers or powder of polypropylene or acrylic fibers were studied. It was thus possible to discriminate formulations that resist spalling from others. For an equivalent given dosage and specific surface, the formulation with the acrylic fibers is found not resistant while that with polypropylene ones were resistant. Thermal analysis showed that the polypropylene melts and vaporizes at relatively low temperatures and the SEM analyses showed that their beds in the concrete are completely freed which may improve connectivity. In contrast, the acrylic fibers do not melt and really tend to leave a plastic film that covers the bed inducing probably a significant reduction of connectivity. In order to discriminate the formulations in general, a critical zone factor, based on the measurement of the pore cumulative volume that must be greater than 0.2 ml / g at 1 MPa pressure, has been defined

## REFERENCES

- [1] Larrad F. D., T. Sedran. 'Optimization of Ultra-High Performance concrete by the use of a packing mode', *Cement and Concrete Research* 24 (6) (1994) 997–1009.
- [2] Sorelli L., Constantinides G., Ulm F.-J., Toutlemonde F., 'The nanomechanical signature of Ultra High Performance Concrete by statistical nanoindentation techniques', *Cement and Concrete Research* 38 (12) (2008) 1447–1456.
- [3] Anderberg Y., 'Spalling phenomena of HPC and OC', in: NIST Workshop on Fire Performance of High Strength Concrete, Gaithersburg, 1997.
- [4] Phan L.T., Lawson J.R., Davis F.L., 'Effects of elevated temperature exposure on heating characteristics, spalling, and residual properties of high performance concrete', *Matériaux et Constructions* 34 (mars 2001) 83–91.
- [5] Bazant Z., Kaplan M. 'Concrete at high temperatures: material properties and mathematical models', Longman, Longman Group Limited Edn. 1996.
- [6] Ulm F.-J., Acker P., Levy M., 'The Chunnel fire. II: Analysis of concrete damage', *Journal of Engineering Mechanics* 125 (3) (1999) 283–289.
- [7] Jansson R., Bostrom L., 'Fire spalling : Theories and experiments', 5th International RILEM Symposium on Self-Compacting Concrete 2 (3/5 sept 2007) 735–740.
- [8] Mindeguia J.-C., Pimienta P., Noumowe A., Kanema M., 'Temperature, pore pressure and mass variation of concrete subjected to high temperature - Experimental and numerical discussion on spalling risk', *Cement and Concrete Research* 40 (2010) 477–487.
- [9] Khoury G., 'Concrete spalling assessment methodologies and polypropylene fibre toxicity analysis in tunnel fires', *Structural concrete* 9 (1) (2008) 11–18.
- [10] Bilodeau A., Kodur V., Hoff G., 'Optimization of the type and amount of polypropylene fibers for preventing the spalling of lightweight concrete subjected to hydrocarbon fire', *Cement and Concrete Composites* 26 (2) (2004) 163–174.
- [11] Hertz K., 'Limits of spalling of fire-exposed concrete', *Fire safety journal* 38 (2003) 103–116.
- [12] Chan Y., Luo X., Sun W., 'Effect of high temperature and cooling regimes on the compressive strength and pore properties of high performance concrete', *Construction and Building Materials* 14 (22 may 2000) 261–266.
- [13] Breitenbrucker R., 'High strength concrete C105 with increased fire resistance due to polypropylene fibres', in: 4th International Symposium on Utilization of High-strength/High-performance concrete, Paris (France), 571–577, 1996.
- [14] Malhotra H., 'The effects of temperature on compressive strength concrete', *Mag Concr Research* 8 (3) (1956) 85–94.

- [15] Liu X., Ye G., De Schutter G., Yuan Y., Taerwe L., ‘On the mechanism of polypropylene fibres in preventing fire spalling in self-compacting and high-performance cement paste’, *Cement and Concrete Research* 38 (20 nov 2007) 487–499.
- [16] Missemer L., « Etude du comportement sous très haute température des Bétons Fibrés à Ultra-Hautes Performances : application au BCV », Thèse de Doctorat, Université de Grenoble, 2011.
- [17] Diamond S., ‘Mercury porosimetry an inappropriate method for the measurement of pore size distribution in cement-based materials’, *Cement and Concrete Research* 30 (10) (2000) 1517–1525.